



**HAL**  
open science

# A multiplicative regularization for force reconstruction

Mathieu Aucejo, Olivier de Smet

► **To cite this version:**

Mathieu Aucejo, Olivier de Smet. A multiplicative regularization for force reconstruction. *Mechanical Systems and Signal Processing*, 2017, 85, pp.730-745. 10.1016/j.ymssp.2016.09.011 . hal-02068499

**HAL Id: hal-02068499**

**<https://hal.science/hal-02068499>**

Submitted on 15 Mar 2019

**HAL** is a multi-disciplinary open access archive for the deposit and dissemination of scientific research documents, whether they are published or not. The documents may come from teaching and research institutions in France or abroad, or from public or private research centers.

L'archive ouverte pluridisciplinaire **HAL**, est destinée au dépôt et à la diffusion de documents scientifiques de niveau recherche, publiés ou non, émanant des établissements d'enseignement et de recherche français ou étrangers, des laboratoires publics ou privés.

# A multiplicative regularization for force reconstruction

M. Aucejo<sup>a</sup>, O. De Smet<sup>a</sup>

<sup>a</sup>*Structural Mechanics and Coupled Systems Laboratory, Conservatoire National des Arts et Métiers, 2 Rue Conté, 75003 Paris, France*

---

## Abstract

Additive regularizations, such as Tikhonov-like approaches, are certainly the most popular methods for reconstructing forces acting on a structure. These approaches require, however, the knowledge of a regularization parameter, that can be numerically computed using specific procedures. Unfortunately, these procedures are generally computationally intensive. For this particular reason, it could be of primary interest to propose a method able to proceed without defining any regularization parameter beforehand. In this paper, a multiplicative regularization is introduced for this purpose. By construction, the regularized solution has to be calculated in an iterative manner. In doing so, the amount of regularization is automatically adjusted throughout the resolution process. Validations using synthetic and experimental data highlight the ability of the proposed approach in providing consistent reconstructions.

*Keywords:* Inverse problem, Force reconstruction, Multiplicative regularization.

---

\*Corresponding author. E-mail address: mathieu.aucejo@lecnam.net

## 1. Introduction

The reconstruction of forces exciting a structure from vibration measurements belongs to the class of ill-posed problems in Hadamard's sense. Practically, this means that such an inverse problem does not necessarily have a unique stable solution. A standard approach to stabilize the inverse problem consists in constraining the space of admissible solutions by including in the formulation of the reconstruction problem some prior information on the distribution of forces to identify. To this end, the inverse problem is generally expressed as a constrained minimization problem. In this theoretical framework, the constraint is defined as a regularization term  $\mathcal{R}(\mathbf{F})$  that encodes prior information on the force distribution  $\mathbf{F}$ . Formally, if  $\mathbf{X}$  is the measured vibration field and  $\mathbf{H}$  is the transfer functions matrix of the studied structure, then the minimization problem may be written:

$$\min_{\mathbf{F}} \mathcal{F}(\mathbf{X} - \mathbf{H}\mathbf{F}) \quad \text{subject to} \quad \mathcal{R}(\mathbf{F}) \leq \beta, \quad (1)$$

where  $\mathcal{F}(\mathbf{X} - \mathbf{H}\mathbf{F})$  is the data fidelity term which controls the a priori on the noise corrupting the data [1, 2] and  $\beta$  is some positive constant [3].

For simplifying its resolution, the previous minimization problem is generally recast into an unconstrained form, in which the regularization term appears as an additive constraint. This particular formulation of the inverse problem is referred to as Tikhonov-like regularization [4, 5] and consists in searching the excitation field  $\mathbf{F}_a$  rendering stationary the functional:

$$J_a(\mathbf{F}, \lambda) = \mathcal{F}(\mathbf{X} - \mathbf{H}\mathbf{F}) + \lambda \mathcal{R}(\mathbf{F}), \quad (2)$$

where  $\lambda$  is the regularization parameter, that controls the balance between data fidelity and regularization terms.

This form of additive regularization has proved its efficiency for reconstructing mechanical forces, as suggested by the extensive literature dedicated to this topic [6, 7, 8, 9, 10, 11, 12]. However, such a regularization is based on the assumption that the regularization parameter  $\lambda$  can be adequately selected. A proper choice of the regularization parameter is all the more crucial as it conditions the quality of the reconstructed solution. That is why, several automatic selection methods have been developed, such as the Morozov's discrepancy principle [13], the Generalized Cross Validation [14], the Unbiased Predictive Risk Estimator [15], the Bayesian estimator [16] or the L-curve method [17]. It can be noted that all these methods generally requires intensive computations, since they are based either on the calculation of the root of some equation, the minimization of some functional or the determination of the maximum curvature of a certain curve.

For the reason mentioned in the previous paragraph, it could be of primary interest to circumvent to this possibly undesirable feature by using a regularization strategy, that eliminates the need for the selection of the optimal regularization parameter before computing the regularized solution. Such a requirement is fulfilled by the multiplicative regularization, originally developed by van den Berg et al. in the context of contrast source inversion [18, 19]. This approach consist in including the regularization term as a multiplicative constraint in the formulation of the inverse problem. As

a consequence, the identified excitation field  $\mathbf{F}_m$  is defined as a stationary point of the functional:

$$J_m(\mathbf{F}) = \mathcal{F}(\mathbf{X} - \mathbf{H}\mathbf{F}) \cdot \mathcal{R}(\mathbf{F}). \quad (3)$$

The multiplicative strategy has been successfully tested in a variety of applications over the past decade, such as microwave imaging [20], image deblurring [21], inverse electromagnetic scattering [22] or geophysics [23].

To the authors' knowledge, the multiplicative regularization has received little attention in the field of structural mechanics. In the present paper, a multiplicative regularization strategy is proposed for reconstructing the forces acting on a structure. It is intended to present a credible alternative to additive regularization, which is the classical choice to solve force reconstruction problems. For this purpose, this paper is divided into five parts, each of them presenting a particular feature of the proposed strategy. In section 2, the main properties of the multiplicative regularization are introduced in order to better explain why such an approach can be used as an alternative for identifying mechanical sources exciting a structure. The formulation of the proposed multiplicative regularization is introduced in section 3, while an iterative algorithm is derived in section 4 to solve the resulting minimization problem. Finally, the ability of the proposed approach in providing consistent reconstructions is illustrated using synthetic and experimental data in sections 5 and 6.

## 2. Main features of the multiplicative regularization

Before presenting the proposed multiplicative regularization into more details, it is worth explaining its main features. To this end, let us consider the simpler form of multiplicative regularization, based on the same data-fidelity and regularization terms as the standard Tikhonov regularization. Formally, this means that one seeks the excitation field  $\mathbf{F}_m$  rendering the functional:

$$J_m(\mathbf{F}) = \|\mathbf{X} - \mathbf{H}\mathbf{F}\|_2^2 \cdot \|\mathbf{F}\|_2^2 \quad (4)$$

stationary. This is equivalent to computing the first-order optimality condition, that is:

$$\left. \frac{\partial J_m(\mathbf{F})}{\partial \mathbf{F}} \right|_{\mathbf{F}=\mathbf{F}_m} = \mathbf{0}. \quad (5)$$

From a practical standpoint, it is convenient to express the previous condition in a more explicit form. After simple algebraic manipulations, Eq. (4) becomes:

$$\mathbf{F}_m = [\mathbf{H}^H \mathbf{H} + \alpha(\mathbf{F}_m) \mathbf{I}]^{-1} \mathbf{H}^H \mathbf{X}, \quad (6)$$

where  $\mathbf{H}^H$  is the hermitian transpose of  $\mathbf{H}$  and  $\alpha(\mathbf{F}_m) = \frac{\|\mathbf{X} - \mathbf{H}\mathbf{F}_m\|_2^2}{\|\mathbf{F}_m\|_2^2}$  defines the regularization parameter of the multiplicative approach [see [Appendix A](#)].

The previous relation clearly shows that the multiplicative approach requires an iterative process to automatically adapt the amount of regularization, since the related regularization parameter  $\alpha(\mathbf{F}_m)$  explicitly depends on the regularized solution  $\mathbf{F}_m$ . For this reason, the parameter  $\alpha$  will be referred to as the adaptive regularization parameter. This particular feature is the primary advantage of the multiplicative regularization over the addi-

tive approach, because it eliminates the need for choosing the regularization parameter  $\lambda$  before computing the regularized solution.

It should however be noted that the multiplicative regularization defined by Eqs. (4) and (5) has one obvious and trivial solution, corresponding to the global minimum of the functional  $J_m(\mathbf{F})$  which is equal to zero:

$$\mathbf{F}_m = \mathbf{0} \quad (\text{i.e. } \alpha(\mathbf{F}_m) \rightarrow +\infty). \quad (7)$$

Generally, this trivial solution is obtained when the noise level is high (typically greater than 20%) [24] or the initial solution is the zero vector. On the other hand, another trivial solution can be obtained when  $\alpha(\mathbf{F}_m) \rightarrow 0$ . In this situation, it is possible to approach the least-squares solution, namely:

$$\mathbf{F}_m \approx \mathbf{H}^+ \mathbf{X}, \quad (8)$$

where  $\mathbf{H}^+ = (\mathbf{H}^H \mathbf{H})^{-1} \mathbf{H}^H$  is the Moore-Penrose pseudoinverse. This solution arises when the noise level is very small (less than 1%) or the initial solution is equal to or too close to this solution. Consequently, these observations highlight the importance of the choice of the solution used to initialize the iterative procedure to avoid these trivial solutions, if they are not the actual solutions of the problem.

Another interesting feature of the multiplicative regularization is that the point  $(\log \|\mathbf{X} - \mathbf{H}\mathbf{F}_m\|_2^2, \log \|\mathbf{F}_m\|_2^2)$  lies on the L-curve [24, 25, 26]. More precisely, this is the point of intersection between the L-curve and a straight line with a slope equal to -1 [see Appendix B]. This property makes the multiplicative and additive regularization strictly equivalent if the regularization

parameter is chosen such that  $\lambda := \alpha(\mathbf{F}_m)$ , as suggested by Eq. (6). Actually, provided that the L-curve exhibits only one corner, the solutions obtain from both strategies slightly differ [24, 26]. In case of multiple corners, the success of the multiplicative regularization strongly depends on the initial guess used to initialize the iterative process [27]. In the end, the multiplicative regularization can be viewed as an a posteriori parameter choice method [25, 26, 27].

However, as it will be made clearer in the next of the paper, it turns out that the multiplicative regularization is computationally less demanding than additive regularization. This difference is mainly due to the estimation of the optimal value of the regularization parameter  $\lambda$ , that is generally performed from automatic selection procedures like the L-curve principle [17]. Indeed, most of these procedures are usually based on the computation of the SVD of  $\mathbf{H}$ , which is known to be computationally expensive.

### 3. Proposed multiplicative regularization

In structural mechanics, forces of different nature can simultaneously excite a structure. One has to notice that, in practical situations, information on both the nature and the location of forces is generally roughly known. Consequently, to aid the reconstruction process in finding a consistent solution, one has to construct a regularization term which properly reflects and exploits this prior information. To this end, suppose that the structure is excited in  $N$  different regions by local excitation fields  $\mathbf{F}_i$  of various types (localized or distributed, for instance). This allows expressing the regularization

term  $\mathcal{R}(\mathbf{F})$  as a sum of local regularization terms  $\tilde{\mathcal{R}}(\mathbf{F}_i)$ , that is:

$$\mathcal{R}(\mathbf{F}) = \sum_{i=1}^N \tilde{\mathcal{R}}(\mathbf{F}_i), \quad (9)$$

where  $\tilde{\mathcal{R}}(\mathbf{F}_i)$  is the regularization term associated to the zone  $i$ . It reflects one's prior knowledge of the nature of the forces in this particular region.

At this stage, it is necessary to specify the expression of the local regularization terms. The main condition they have to satisfy is to be flexible enough to reflect different priors. This requirement is fulfilled by the following regularization term:

$$\tilde{\mathcal{R}}(\mathbf{F}_i) = \|\mathbf{L}_i \mathbf{F}_i\|_{q_i}^{q_i}, \quad (10)$$

where  $q_i$  is a tuning parameter included in the interval  $]0, +\infty[$ ,  $\|\bullet\|_{q_i}$  is the  $\ell_{q_i}$ -norm or quasi-norm and  $\mathbf{L}_i$  is a smoothing operator controlling the regularity of the solution in the zone  $i$ .

To properly choose the value of the tuning parameter  $q_i$  in each zone, it can be noticed from Fig. 1 that the smaller  $q_i$  is, the larger is the weight on small values of  $\mathbf{L}_i \mathbf{F}_i$ . On the contrary, for large values of  $\mathbf{L}_i \mathbf{F}_i$ , the smaller  $q_i$  is, the smaller is the weight on these values. This difference in the weighting behavior for small and large values of  $\mathbf{L}_i \mathbf{F}_i$  can be directly observed in the solutions obtained, since for  $q_i \leq 1$  the solution vector  $\mathbf{L}_i \mathbf{F}_{\mathbf{m}i}$  will tend to have only a few non-zero values, while for  $q_i = 2$  it will tend to have only a few very small values. From this analysis, it can be inferred that distributed sources are promoted for  $q_i = 2$  and  $\mathbf{L}_i = \mathbf{I}$ , while localized sources are favored for  $q_i \leq 1$  and  $\mathbf{L}_i = \mathbf{I}$ . For promoting piecewise continuous solutions, one can set

$q_i \leq 1$  and define the smoothing operator  $\mathbf{L}_i$  as the discretized form of the  $n^{\text{th}}$ -order differential operator using the corresponding finite difference scheme [28]. Thus, the solution  $\mathbf{F}_{\text{mi}}$  is approximated by piecewise constant segments if  $n = 1$ , while the solution is approximated by piecewise polynomials of degree 1 if  $n = 2$  [29].

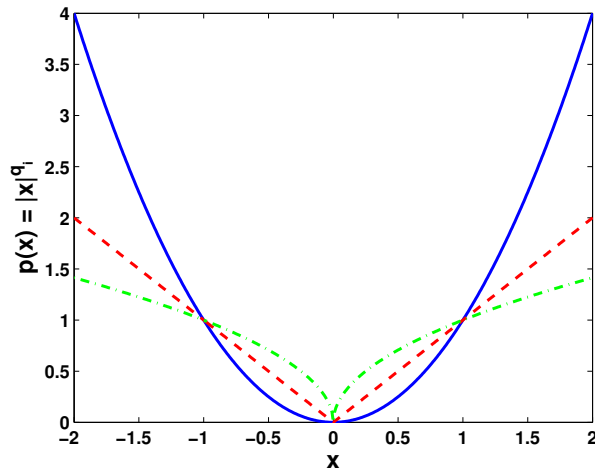


Figure 1: Penalty function  $p(x) = |x|^{q_i}$  associated to the regularization term for (—)  $q_i = 2$ , (---)  $q_i = 1$  and (-.-)  $q_i = 0.5$

To complete the formulation of the multiplicative regularization, one has to define the data fidelity term. As classically assumed in the literature, if one supposes that the vibration field  $\mathbf{X}$  is corrupted by an additive Gaussian white noise, it is reasonable to express the data fidelity term such that:

$$\mathcal{F}(\mathbf{X} - \mathbf{HF}) = \|\mathbf{X} - \mathbf{HF}\|_2^2. \quad (11)$$

Finally, by introducing Eqs. (10) and (11) into Eq. (3), one obtains the

general expression of the functional  $J_m(\mathbf{F})$ :

$$J_m(\mathbf{F}) = \|\mathbf{X} - \mathbf{H}\mathbf{F}\|_2^2 \cdot \sum_{i=1}^N \|\mathbf{L}_i \mathbf{F}_i\|_{q_i}^{q_i}. \quad (12)$$

It should be noted that the data fidelity and regularization terms defined in Eqs. (10) and (11) have been used by the authors in a previous work to derive the additive version of the proposed multiplicative regularization [12]. Results obtained in this earlier work have demonstrated that such data fidelity and regularization terms are well adapted to address the force reconstruction problem. That is why, similar conclusions are expected with the proposed multiplicative strategy.

#### 4. Resolution of the inverse problem

The resolution of the reconstruction problem defined by the multiplicative regularization presented in section 3 requires the implementation of an iterative procedure. As already evoked in section 2, it is mainly related to the specificity of the multiplicative regularization consisting in adaptively determining the amount of regularization throughout the resolution process. On the other hand, the definition of an iterative algorithm is all the more necessary that the solution of a reconstruction problem involving  $\ell_{q_i}$ -norms has generally no closed-form expression.

To properly handle both issues, it is proposed to implement an Iteratively Reweighted Least-Squares (IRLS) scheme. Such an iterative procedure has already been successfully used in previous studies to solve force reconstruction problems written in the form of an additive regularization [11, 12]. In

the next of this section, an adapted version of this algorithm is introduced to deal with the proposed multiplicative strategy.

#### 4.1. General principles

The basic idea behind the IRLS algorithm is to replace the direct calculation of the stationary point of the functional  $J_m(\mathbf{F})$  [see Eq. (12)], by an equivalent iterative process having an explicit and unique solution at each iteration. For this purpose, the  $\ell_{q_i}$ -norm has to be recast into a weighted  $\ell_2$ -norm. In doing so, it is expected that solution of the iterative process converges to the solution of the proposed multiplicative strategy.

The direct application of this idea to the proposed regularization problem leads to define the estimated force vector  $\mathbf{F}_m^{(k+1)}$  at iteration  $k+1$  as the vector rendering stationary the functional:

$$J_m^{(k+1)}(\mathbf{F}) = \|\mathbf{X} - \mathbf{H}\mathbf{F}\|_2^2 \cdot \sum_{i=1}^N \left\| \mathbf{W}_i^{(k)1/2} \mathbf{L}_i \mathbf{F}_i \right\|_2^2, \quad (13)$$

where  $\mathbf{W}_i^{(k)}$  is a local weighting definite positive diagonal matrix.

As classically done in IRLS-type algorithm, the weighting matrices  $\mathbf{W}_i^{(k)}$  are defined such that:

$$\mathbf{W}_i^{(k)} = \text{diag} \left[ w_{i,1}^{(k)}, \dots, w_{i,j}^{(k)}, \dots, w_{i,N_i}^{(k)} \right] = \begin{bmatrix} w_{i,1}^{(k)} & & 0 \\ & \ddots & \\ 0 & & w_{i,N_i}^{(k)} \end{bmatrix} \quad (14)$$

with:

$$w_{i,j}^{(k)} = \max \left( \epsilon_i, \left| f_j^{(k)} \right| \right)^{q_i-2}, \quad (15)$$

where  $N_i$  is the number of identification points in the zone  $i$ ,  $f_j^{(k)}$  is the  $j^{\text{th}}$  component of the vector  $\mathbf{L}_i \mathbf{F}_{\mathbf{m}i}^{(k)}$  and  $\epsilon_i$  is a small real positive number acting as a damping parameter. It allows avoiding infinite weights when  $\left| f_j^{(k)} \right| \rightarrow 0$  and  $q_i < 2$ . Practically, the damping parameter is automatically selected once for all during the initialization step from the cumulative histogram of  $\left| \mathbf{L}_i \mathbf{F}_{\mathbf{m}i}^{(0)} \right|$ . More precisely, its value is chosen so that 5% of the values of  $\left| \mathbf{L}_i \mathbf{F}_{\mathbf{m}i}^{(0)} \right|$  are less than or equal to  $\epsilon_i$  [11, 30].

For implementation convenience, Eq. (13) should be expressed in a more compact form by introducing two matrices,  $\mathbf{W}^{(k)}$  and  $\mathbf{L}$ , defined as follows:

$$\mathbf{W}^{(k)} = \text{diag} \left( \mathbf{W}_1^{(k)}, \dots, \mathbf{W}_N^{(k)} \right) \quad \text{and} \quad \mathbf{L} = \text{diag} \left( \mathbf{L}_1, \dots, \mathbf{L}_N \right). \quad (16)$$

The introduction of the global matrices  $\mathbf{W}^{(k)}$  and  $\mathbf{L}$  into Eq. (13) allows writing the functional  $J_m^{(k+1)}(\mathbf{F})$  at iteration  $k+1$  under the following generic form:

$$J_m^{(k+1)}(\mathbf{F}) = \|\mathbf{X} - \mathbf{H}\mathbf{F}\|_2^2 \cdot \left\| \mathbf{W}^{(k)1/2} \mathbf{L}\mathbf{F} \right\|_2^2. \quad (17)$$

An additional step is finally required to obtain the operational form of the previous minimization problem. After some simple calculations, one gets the following explicit expression:

$$\mathbf{F}_{\mathbf{m}}^{(k+1)} = \left( \mathbf{H}^H \mathbf{H} + \alpha^{(k+1)} \mathbf{L}^H \mathbf{W}^{(k)} \mathbf{L} \right)^{-1} \mathbf{H}^H \mathbf{X}, \quad (18)$$

where the adaptive regularization parameter  $\alpha^{(k+1)}$  is defined such that:

$$\alpha^{(k+1)} = \frac{\left\| \mathbf{X} - \mathbf{H}\mathbf{F}_{\mathbf{m}}^{(k)} \right\|_2^2}{\left\| \mathbf{W}^{(k)1/2} \mathbf{L}\mathbf{F}_{\mathbf{m}}^{(k)} \right\|_2^2}. \quad (19)$$

#### 4.2. Choice of the initial guess and stopping criterion

The proposed resolution algorithm being iterative, the present section aims at introducing the choices of the initial guess and the stopping criterion.

##### 4.2.1. Choice of the initial guess

It is clear from section 3 that the proposed multiplicative formulation is generally non-convex, meaning that the existence of a unique minimizer is not guaranteed. Consequently, the choice of a good initial guess  $\mathbf{F}_m^{(0)}$  is crucial for a successful reconstruction.

A good initial guess can be defined as a coarse solution of the problem, easy to compute, but sufficiently close to the solution to ensure the convergence of the iterative process. Such a requirement is fulfilled by the solution of a standard Tikhonov-like regularization, that is:

$$\mathbf{F}_m^{(0)} = (\mathbf{H}^H \mathbf{H} + \alpha^{(0)} \mathbf{L}^H \mathbf{L})^{-1} \mathbf{H}^H \mathbf{X}, \quad (20)$$

where  $\alpha^{(0)}$  is a rough estimate of the converged value of the adaptive regularization parameter or, equivalently, of the value of the regularization parameter  $\lambda$  picked by the L-curve method.

The parameter  $\alpha^{(0)}$  has to be ideally determined without using any selection procedures or large computational efforts in order to preserve the advantage of the multiplicative strategy. This task proves to be difficult in practice, because the order of magnitude of the optimal regularization parameter is a priori unknown from the data only. However, one has to notice that the optimal regularization parameter is generally comprised between the smallest and the largest singular values of  $\mathbf{A} = [\mathbf{H}\mathbf{L}^{-1}]^H [\mathbf{H}\mathbf{L}^{-1}]$ . From this

observation and a series of numerical experiments, we propose a heuristic rule for determining  $\alpha^{(0)}$ , that limits the computational efforts and leads to consistent identified solutions. The proposed estimation procedure is divided into three steps:

1. Find estimates of the largest and the smallest singular values of  $\mathbf{A}$ , noted  $\hat{\sigma}_1$  and  $\hat{\sigma}_n$  respectively.

The estimate of the largest singular value is given by the upper bound of  $\sigma_1$ , namely [31]:

$$\hat{\sigma}_1(\mathbf{A}) = \sqrt{\|\mathbf{A}\|_\infty \|\mathbf{A}\|_1}. \quad (21)$$

The estimation of the smallest singular value is obtained from  $\hat{\sigma}_1$  and an estimate  $\hat{\kappa}$  of the condition number of  $\mathbf{A}$ , namely:

$$\hat{\sigma}_n(\mathbf{A}) = \frac{\hat{\sigma}_1(\mathbf{A})}{\hat{\kappa}(\mathbf{A})}. \quad (22)$$

2. Define a set  $S_{\alpha_0}$  of possible values of  $\alpha^{(0)} \in [\hat{\sigma}_n, \hat{\sigma}_1]$  using a constant logarithmic spacing to take into account the decrease of the singular values.
3. Choose  $\alpha^{(0)} = \text{median}(S_{\alpha_0})$ .

Because this estimation procedure is heuristic, it may sometimes fail to give a good starting point for the iterative process. In such a situation, it is always possible to choose  $\alpha^{(0)}$  as the regularization parameter picked by the L-curve. Incidentally, the computational efficiency of the overall procedure is affected in proportion to the size of the transfer functions matrix.

#### 4.2.2. Choice of the stopping criterion

The proposed iterative algorithm offers a natural definition of the stopping criterion, based on the relative variation of the adaptive regularization parameter between two successive iterations. In the present paper, the relative variation  $\delta$  of the adaptive regularization parameter is defined such that:

$$\delta = \frac{|\alpha^{(k+1)} - \alpha^{(k)}|}{\alpha^{(k)}}. \quad (23)$$

As classically done in the literature, the iterative process is stopped when the relative variation  $\delta$  is less than or equal to some tolerance. Experimentally, it has been found that setting the tolerance to  $10^{-8}$  allows obtaining consistent reconstructions.

#### 4.3. Generic resolution algorithm

To clearly highlight each step of the proposed iterative process, a detailed generic version is given in table 1.

### 5. Numerical validation

The numerical study of the proposed multiplicative regularization has two main purposes. First of all, it aims at highlighting the particular interest of properly exploiting one's prior knowledge of the nature and locations of the sources to identify. Second, it is intended to provide a fair comparison of the performance of the proposed approach with its additive counterpart, in order to clearly reveal the practical advantage of the multiplicative approach.

Table 1: Generic resolution algorithm

---

**Inputs:** Transfer functions matrix  $\mathbf{H}$ , Measured vibration field  $\mathbf{X}$ ,  
Selected zones  $\{i\}$ , Differentiation matrix  $\mathbf{L}$ , Tolerance  $tol$

**Output:** Reconstructed force vector  $\mathbf{F}_m$

**Initialization:** Compute  $\alpha^{(0)}$  from procedure described in sec. 4.2.1  
Compute  $\mathbf{F}_m^{(0)}$  from Eq. (20)  
Compute  $\epsilon_i$  from the cumulative histogram of  $|\mathbf{L}_i \mathbf{F}_{mi}^{(0)}|$   
Initialize  $\delta$  to 1  
Initialize  $k$  to 0

**Iteration:**

**while**  $\delta > tol$

Compute  $\mathbf{W}_i^{(k)}$  from Eq. (14)

Construct  $\mathbf{W}^{(k)}$  from Eq. (16)

Compute  $\alpha^{(k+1)}$  from Eq. (19)

Compute  $\mathbf{F}_m^{(k+1)}$  from Eq. (18)

Update  $\delta$  using Eq. (23)

$k \leftarrow k + 1$

**end**

**return**  $\mathbf{F}_m \leftarrow \mathbf{F}_m^{(k)}$

---

### 5.1. Description of the test case

In the present numerical validation, one seeks to identify a point force of unit amplitude acting on a thin simply supported steel plate with dimensions  $0.6 \times 0.4 \times 0.005 \text{ m}^3$ . The coordinates of the point force, measured from the lower left corner of the plate, are  $(x_0, y_0) = (0.42 \text{ m}, 0.25 \text{ m})$ . Practically, this configuration allows studying the influence of the definition of local regularization terms, since the present excitation field exhibits two types of spatial distribution over the structure, namely a smooth distribution of the reaction forces at boundaries and a singular distribution around the location of the point force.

To properly simulate experimental measurements, the exact vibration displacement field  $\mathbf{X}_{\text{exact}}$  is first computed from a FE mesh of the plate made up with 187 shell elements, assuming that only bending motions are measurable. Then, the exact displacement field is corrupted by an additive Gaussian white noise with a signal-to-noise ratio equal to 30 dB. It should be added that a structural damping has been introduced in the calculation to avoid infinite displacement amplitudes at resonance frequencies. Here, the structural damping ratio is equal to 0.01.

Regarding, finally, the transfer functions matrix  $\mathbf{H}$ , a FE model of the plate with free boundary conditions is used, assuming that only bending motions are measured. In other words, the computed transfer functions matrix  $\mathbf{H}$  is dynamically condensed over the measurable dofs only [11, 32]. The main interest in using free boundary conditions to model the dynamic behavior of

the plate is to allow the identification of external excitations acting on the structure as well as reaction forces at boundaries [10].

### 5.2. Application of the proposed multiplicative regularization

To assess the ability of the proposed multiplicative strategy in providing consistent reconstructions, it is first necessary to define the reference force vector  $\mathbf{F}_{\text{ref}}$  that could serve as a proper benchmark. This reference force vector is computed from the transfer functions matrix  $\mathbf{H}$  and the exact displacement field  $\mathbf{X}_{\text{exact}}$  thanks to the following relation:

$$\mathbf{F}_{\text{ref}} = \mathbf{H}^{-1} \mathbf{X}_{\text{exact}}. \quad (24)$$

Let us begin this numerical study with the identification of the excitation field at 500 Hz, i.e. outside the resonance frequencies of the plate. As shown in Fig. 2, the reference force vector corresponds to the description of the test case given in the previous section, since it exhibits smooth reaction forces at boundaries of the plate as well as a unit point force at  $(x_0, y_0) = (0.42 \text{ m}, 0.25 \text{ m})$ .

A naive identification of the force vector  $\mathbf{F}_{\text{naive}}$  is obtained by replacing the exact vibration field by the corrupted one in Eq. (24). As shown in Figure 3, the reconstruction fails, since the identified excitation field is highly dominated by the noise. This disappointing result is related to the presence of small singular values in  $\mathbf{H}$  causing the amplification of the noise vector components in the reconstructed solution [28].

A classical idea to stabilize the inverse problem consist in defining a regularization term that reflects a global a priori on the nature and the spatial distribution of excitation forces. Obviously, such a regularization requires

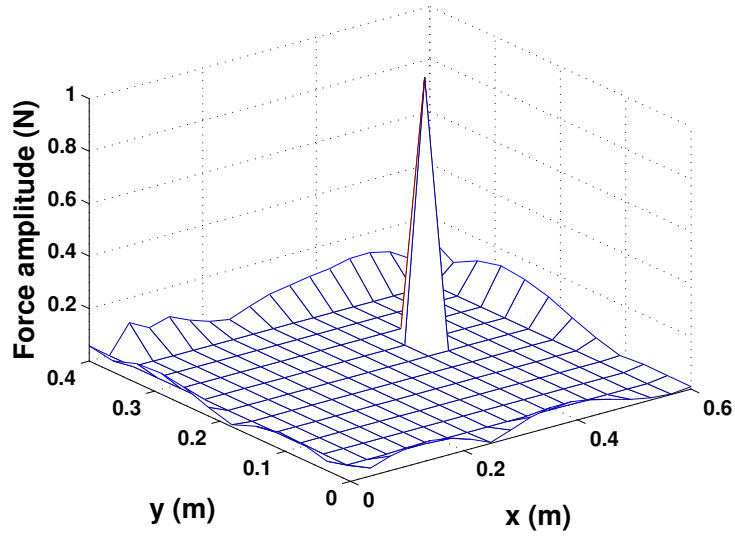


Figure 2: Reference force vector  $\mathbf{F}_{\text{ref}}$  at 500 Hz

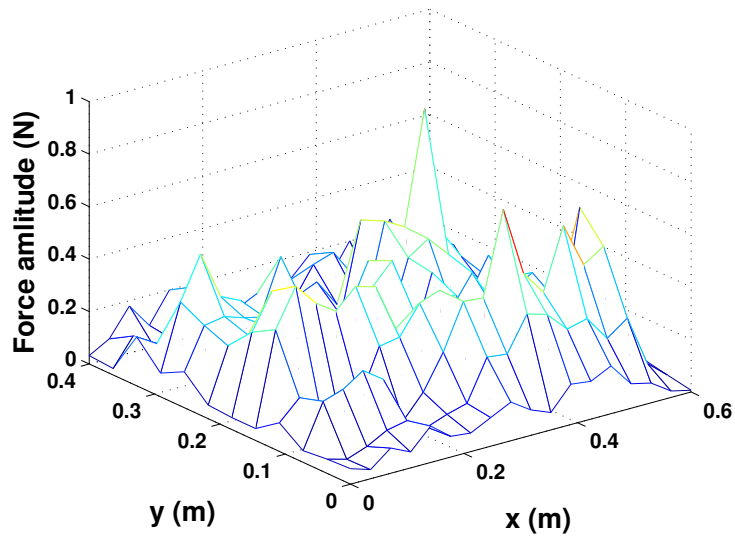


Figure 3: Naive reconstruction of the force vector  $\mathbf{F}_{\text{naive}}$  at 500 Hz

to carefully establish a compromise between the smoothness of the reaction forces at boundaries and the singularity of the point force. However, the regularization term being fully adapted neither to localized sources nor distributed sources, one can infer that the reconstructed excitation field can not perfectly match the actual one. This remark is illustrated in Figure 4 presenting the reconstructed excitation field from a global regularization term of the form of Eq. (10) for  $q = 1.1$  and  $\mathbf{L} = \mathbf{I}$ . This particular choice provides a relevant reconstruction, since the identified point force  $F_{m0}$  is equal to 0.96 N instead of 1 N, while the reaction forces are in good agreement with the reference ones. However, the choice of the tuning parameter is not obvious and requires a great expertise, which is not desirable for an identification procedure.

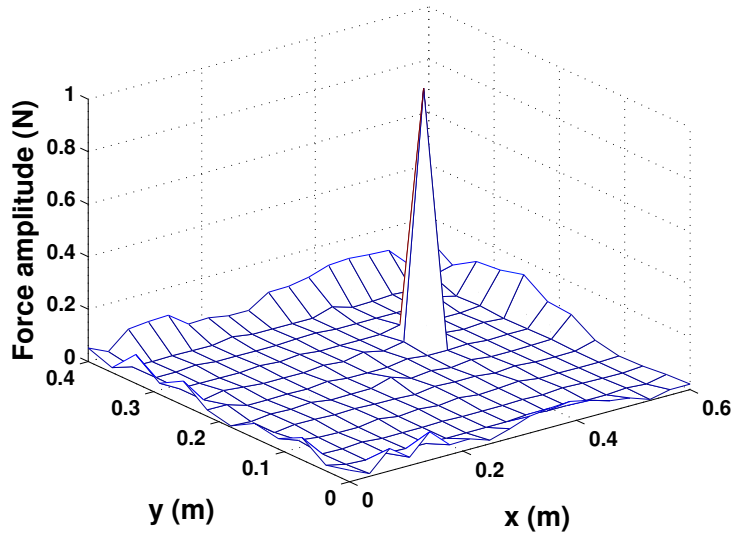


Figure 4: Reconstructed force vector  $\mathbf{F}_m$  at 500 Hz from corrupted data using a global regularization term -  $q = 1.1$  and  $\mathbf{L} = \mathbf{I}$

The previous results better explain the need for properly exploiting one's prior knowledge of the nature and the location of excitation sources. To obtain a better reconstruction, one has to notice that the force vector to identify is sparse except at the boundaries of the plate [see Fig. 2]. This observation leads to define the two reconstruction zones plotted in Fig. 5: (i) a central region associated to the tuning parameter  $q_1$  and containing the point force only, in which a sparsity-promoting prior has to be employed, and (ii) a region associated to the tuning parameter  $q_2$  and corresponding to the boundaries of the plate, in which a prior promoting smooth solutions is required.

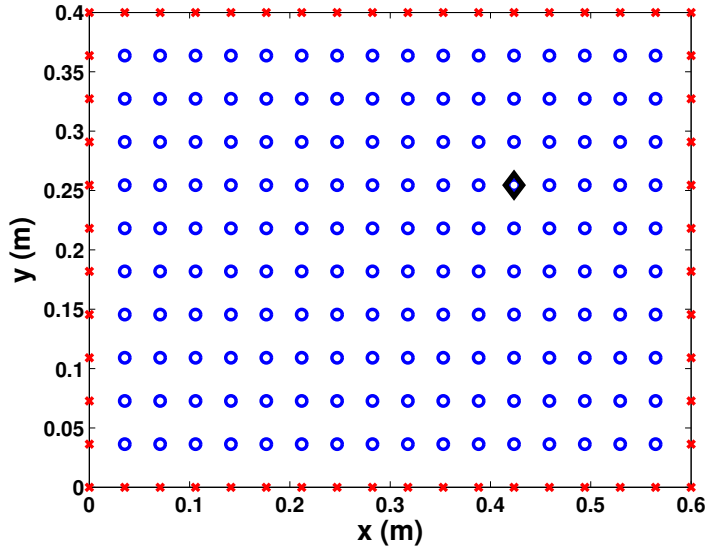


Figure 5: Definition of the reconstruction zones - ( $\circ$ ) zone 1 (sparse), ( $\times$ ) zone 2 (smooth) and ( $\diamond$ ) location of the point force

From the explanations given in section 3, it is reasonable to set  $(q_1, q_2) = (0.5, 2)$ . The resulting reconstructed force vector is presented in Fig. 6. It

can be seen that the reconstruction is successful, since the reconstructed force vector is very similar to the reference one. In particular, it is noteworthy that the identified point force amplitude  $F_{m0}$  is equal to 0.998 N instead of 1 N.

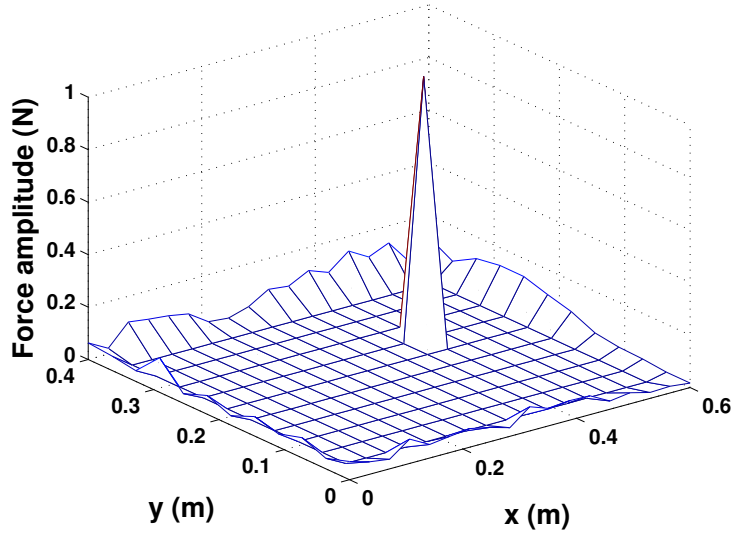


Figure 6: Reconstructed force vector  $\mathbf{F}_m$  at 500 Hz from corrupted data when using local priors on the spatial distribution of the excitation field -  $(q_1, q_2) = (0.5, 2)$  and  $\mathbf{L} = \mathbf{I}$

The analysis presented above has been performed outside the resonance frequencies of the plate. However, force reconstruction at natural frequencies of a lightly damped structure is known to be far more difficult, since at these frequencies the shape of the vibration response of the structure is close to that of the corresponding mode shape. In other words, the vibration response is mainly driven by boundary forces and not by the point force itself. From the standpoint of the identification process, this can be regarded as an increase of the noise level. To assess the ability of the multiplicative strategy in providing consistent reconstructions at natural frequencies of the

structure, the identification procedure is applied on the test case described previously at 378 Hz, 720 Hz and 915 Hz. The corresponding identifications are presented in Fig. 7. Obtained results show that for each natural frequency the shape of the identified force vector is consistent with the reference one, although the amplitude of the identified point force  $F_{m0}$  is generally slightly underestimated. Indeed, the identified amplitude is equal on average to 0.912 N instead of 1 N. Nevertheless, these results show that the proposed method allows having credible information on the sources acting on the structure at resonance frequencies.

### 5.3. Comparison with the related additive regularization

The additive counterpart of the proposed multiplicative regularization has been developed in [11]. Practically, the reconstructed force vector  $\mathbf{F}_a$  is the vector that renders stationary the functional:

$$J_a(\mathbf{F}, \lambda) = \|\mathbf{X} - \mathbf{H}\mathbf{F}\|_2^2 + \lambda \sum_{i=1}^N \|\mathbf{L}_i \mathbf{F}_i\|_{q_i}^{q_i}. \quad (25)$$

As for the present multiplicative regularization, the previous additive approach is solved using an IRLS scheme. The main differences between the both versions of this iterative process lie in the calculation of the initial solution and the solution at iteration  $k+1$ . Indeed, for the additive strategy, the initial solution writes:

$$\mathbf{F}_a^{(0)}(\lambda) = (\mathbf{H}^H \mathbf{H} + \lambda^{(0)} \mathbf{L}^H \mathbf{L})^{-1} \mathbf{H}^H \mathbf{X}, \quad (26)$$

while the solution at iteration  $k+1$  is defined such that:

$$\mathbf{F}_a^{(k+1)}(\lambda) = \left( \mathbf{H}^H \mathbf{H} + \lambda^{(k+1)} \mathbf{L}^H \mathbf{W}^{(k)} \mathbf{L} \right)^{-1} \mathbf{H}^H \mathbf{X}, \quad (27)$$

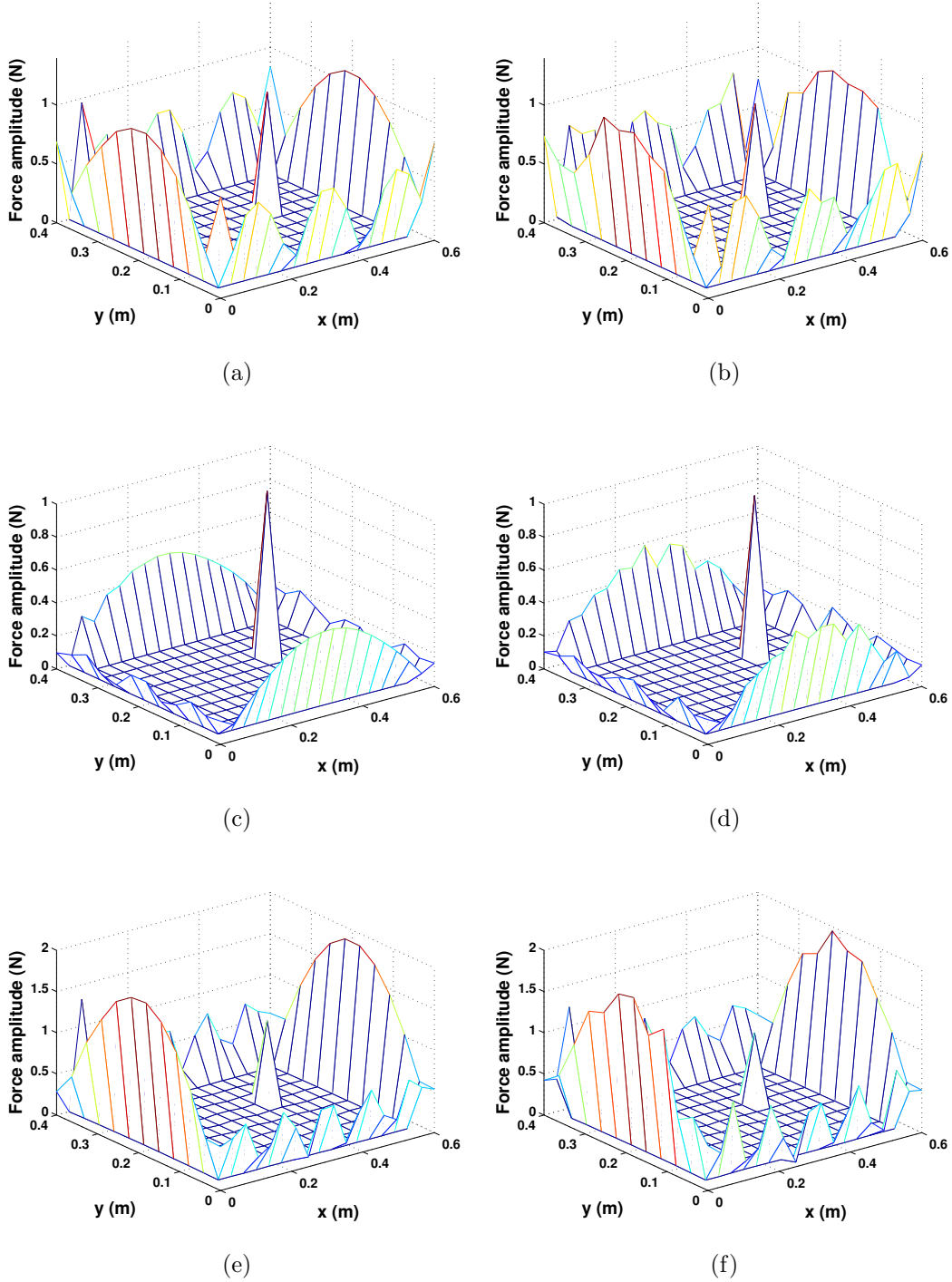


Figure 7: Identification of the force vector  $\mathbf{F}_{\mathbf{I}_m}$  at resonance frequencies of the structure - (a) Reference at 378 Hz, (b) Identification at 378 Hz, (c) Reference at 720 Hz, (d) Identification at 720 Hz, (e) Reference at 915 Hz and (f) Identification at 915 Hz -  $(q_1, q_2) = (0.5, 2)$  and  $\mathbf{L} = \mathbf{I}$

where  $\lambda^{(0)}$  and  $\lambda^{(k+1)}$  are respectively the initial and the updated regularization parameters computed using the L-curve principle. This strategy is referred to as updated additive regularization.

To fairly compare previous additive and multiplicative regularization strategies, one first proposes to reconstruct the excitation field at 100 Hz using the same input data, namely the same transfer functions matrix  $\mathbf{H}$ , the same corrupted vibration field  $\mathbf{X}$  and the same tuning parameters  $(q_1, q_2)$ . The corresponding reconstructions are presented in Figs. 8b and 8c. It is interesting to note that both reconstructed force vectors are close together and similar to the reference one. In particular, one can notice that the identified point force amplitudes  $F_{a0}$  and  $F_{m0}$  are respectively equal to 0.93 N and 0.94 N instead of 1 N. Actually, the major difference between both calculations lies in the number of iterations and the elapsed time to reach the convergence. Indeed, the additive regularization requires 16 iterations and 1.45 s to converge, while the multiplicative version needs 27 iterations but only 0.11 s. It is worth highlighting that even though the multiplicative regularization requires more iterations than the additive one, it is generally faster. As already evoked in section 2, this can easily be explained by the fact that the selection procedure used to determine the values of the regularization parameters  $\lambda^{(0)}$  and  $\lambda^{(k+1)}$  is based on the computation of SVD (or the GSVD) of the system. This observation is corroborated by the results presented in table 2, where the elapsed time of the operations that differ between the algorithms used to compute  $\mathbf{F}_m$  and  $\mathbf{F}_a$  are given. As a side note, the running times of the proposed initialization procedure [see section 4.2.1] and the SVD

implemented in Matlab<sup>®</sup> are appraised with respect to the size of the problem in [Appendix C](#) in order to fairly compare both regularization algorithms.

Table 2: Comparison of the elapsed time ( $t_e$ ) of the operations differing in the algorithms used to compute  $\mathbf{F}_m$  and  $\mathbf{F}_a$  - *The elapsed time given for the update step corresponds to an average time over all the iterations*

Operations	Mult. reg.	Updated add. reg.
	$t_e$ (s)	$t_e$ (s)
Initialization ( $\alpha^{(0)}$ or $\lambda^{(0)}$ )	$1.6 \times 10^{-2}$	$6.0 \times 10^{-2}$
Update ( $\alpha^{(k+1)}$ or $\lambda^{(k+1)}$ )	$7.5 \times 10^{-4}$	$6.0 \times 10^{-2}$

This trend is confirmed in table 3, where the identified point force amplitude, the number of iterations and the elapsed time are given for both strategies and several frequencies. The results presented in table 3 clearly show that the multiplicative approach is significantly faster than the additive strategy to obtain similar values of the point force amplitude. In the present case, the multiplicative regularization is about 10 times faster than the related additive regularization.

However, one can argue that the regularization parameter may be chosen once for all during the initialization step of the iterative procedure by setting  $\lambda^{(k+1)} = \lambda^{(0)}$  [11, 12]. Practically, this non-updated version has the great advantage of decreasing the computation time of the regularization process, since the regularization parameter, and so the SVD of the system, is com-

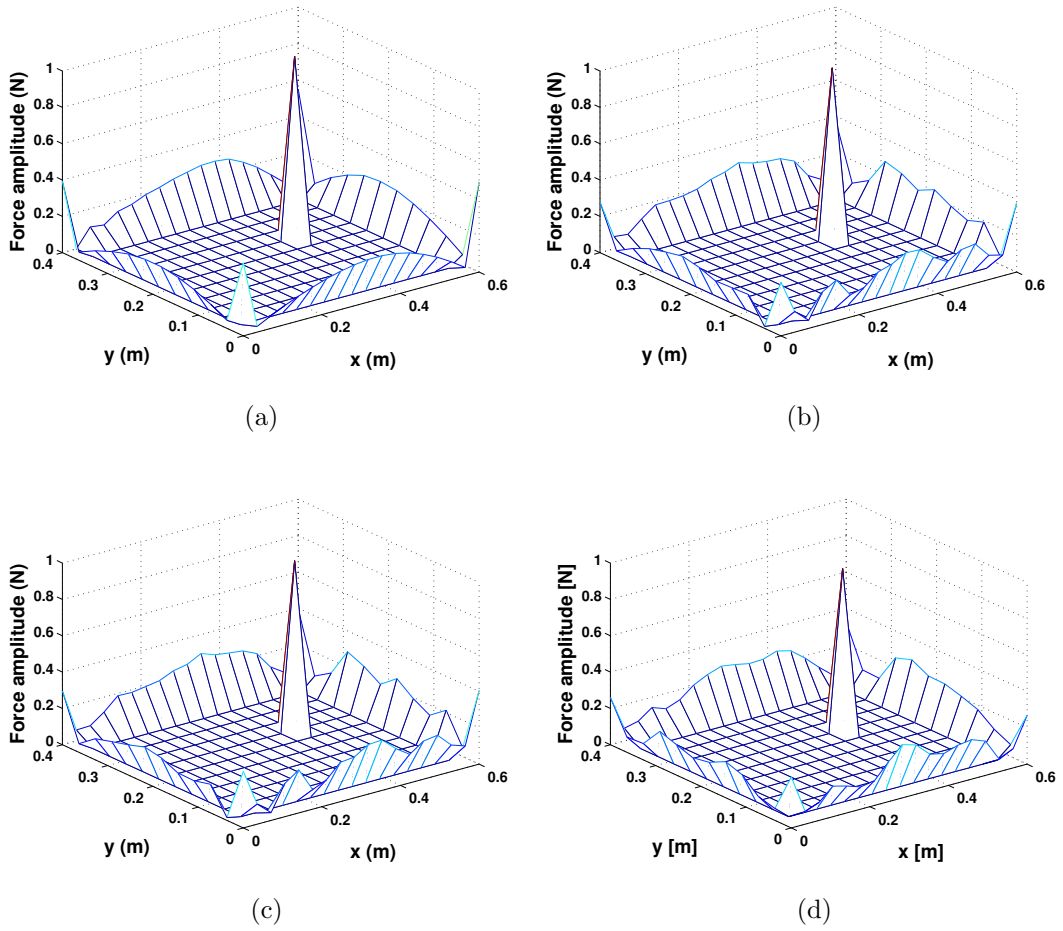


Figure 8: Comparison of multiplicative and additive regularization strategies at 100 Hz from the same corrupted vibration data, the same tuning parameters  $(q_1, q_2) = (0.5, 2)$  and the same differentiation matrix  $\mathbf{L} = \mathbf{I}$  - (a) Reference, (b) Multiplicative regularization, (c) Updated additive regularization and (d) Non-updated additive regularization

Table 3: Comparison of the multiplicative regularization and the updated additive regularization with updated regularization parameter -  $F_{m0}$  or  $F_{a0}$ : identified point force amplitude (N),  $N_{it}$ : number of iterations,  $t_e$ : elapsed time (s)

Frequency	Mult. reg.			Updated add. reg.		
	$F_{m0}$	$N_{it}$	$t_e$	$F_{a0}$	$N_{it}$	$t_e$
100 Hz	0.940	27	0.11	0.930	14	1.45
378 Hz	0.912	16	0.08	0.868	14	1.38
500 Hz	0.998	15	0.11	0.996	8	0.98
720 Hz	0.971	27	0.11	0.970	10	1.14
915 Hz	0.855	18	0.08	0.842	12	1.34
1000 Hz	0.997	26	0.11	0.996	8	0.93

puted only once. In this case, it is clear from Fig. 8d and table 4 that such additive regularization exhibits time performances and identified solutions roughly similar to the multiplicative approach. It should, however, be noticed that the corresponding identified point force amplitudes are lower than those estimated with the multiplicative strategy.

## 6. Experimental validation

This section aims at confirming the main conclusions drawn in the previous section by extending the analysis to a real-world application. More specifically, it is expected to highlight the need for updating the regularization parameter throughout the iterative process and subsequently the practical interest of the multiplicative regularization compared to the more classical

Table 4: Comparison of the multiplicative regularization and the non-updated additive regularization without updating the regularization parameter -  $F_{i0}$ : identified point force amplitude (N),  $N_{it}$ : number of iterations,  $t_e$ : elapsed time

Frequency	Mult. reg.			Non-updated add. reg.		
	$F_{m0}$	$N_{it}$	$t_e$	$F_{a0}$	$N_{it}$	$t_e$
100 Hz	0.940	27	0.11	0.888	18	0.13
378 Hz	0.912	16	0.08	0.857	15	0.15
500 Hz	0.998	15	0.11	0.982	11	0.13
720 Hz	0.971	27	0.11	0.940	11	0.12
915 Hz	0.855	18	0.08	0.756	13	0.13
1000 Hz	0.997	26	0.11	0.953	11	0.13

additive approach.

### 6.1. Description of the experimental set-up

The structure under test is a suspended (free) aluminum plate of 0.6 m in length, 0.4 m in width and 5 mm in thickness [see Fig. 9a]. The plate is excited at  $(x_0, y_0) = (0.405 \text{ m}, 0.255 \text{ m})$  by a shaker fed by a white noise signal and equipped with a force sensor [see Fig. 9b].

Measurements of the vibration field were carried out with a scanning laser vibrometer on a grid of  $35 \times 29$  points along x and y directions respectively using the force signal as phase reference. Regarding the FE mesh used to model the dynamic behaviour of the plate, it has been designed to perfectly match the measurement mesh. As a result, it consists of 952 shell elements,

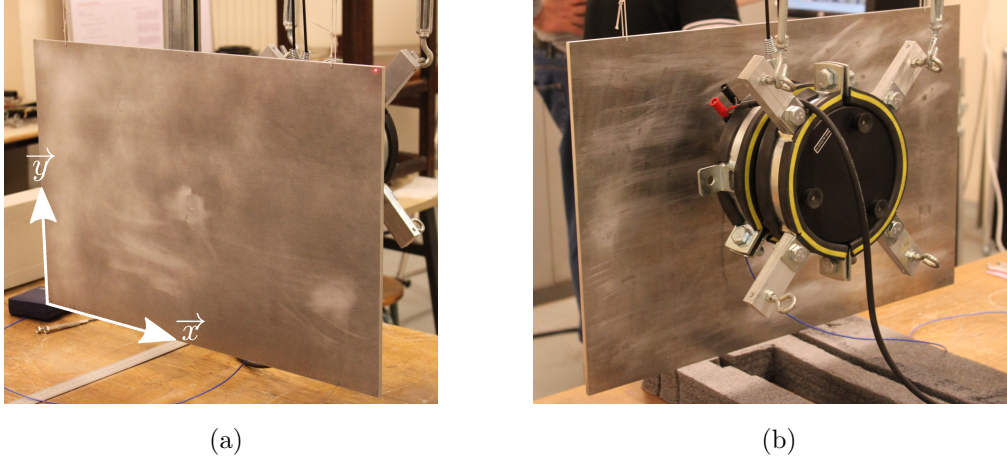


Figure 9: Experimental set-up - (a) Suspended plate and (b) Excitation device

making the model theoretically valid up to 4500 Hz. Then, the corresponding FE model with free boundary conditions has been used to compute the transfer functions matrix  $\mathbf{H}$ , considering the bending motions as the only available data. Finally, it is worth noting that a global structural damping is used in the present experimental validation. Its value has been estimated from the modal damping ratios obtained from the measured FRFs.

### 6.2. Application

In the numerical validation, the proposed multiplicative regularization has been compared to the related additive regularization by either updating the value of the regularization parameter at each iteration or using a unique value calculated during the initialization of the IRLS algorithm. We propose to follow a similar analysis process in this section.

The analysis of the experimental set-up suggests the definition of a sole

identification region corresponding to the whole surface of the plate. In addition, the target excitation field being very sparse, the tuning parameter  $q$  is set to 0.5 according to the rule of thumb given in section 3.

Table 5 gathers results identified at  $(\hat{x}_0, \hat{y}_0) = (0.404 \text{ m}, 0.256 \text{ m})$  by the multiplicative and additive regularizations for two resonance frequencies (196.25 Hz and 1161.25 Hz) and two non-resonant frequencies (725 Hz and 1500 Hz). As expected from the numerical validation, the point force amplitudes produced by the multiplicative and the updated additive regularizations are consistent with the target values, but, in all cases, the multiplicative approach is more efficient in terms of computation time. Actually, more surprising results are obtained for the non-updated additive regularization, because it always fails in recovering the point force amplitude. This deficiency of the non-updated version clearly appears when displaying the reconstructed excitation field at a particular frequency. For instance, Fig. 10 shows that the excitation field identified at 196.25 Hz by the non-updated additive regularization has no physical meaning, while those reconstructed from the other two strategies succeed in both localizing and quantifying the point force. This apparent contradiction between the numerical and experimental studies arises because the ratios  $\lambda^{(0)}/\alpha^{(N_{it})}$  and  $\lambda^{(0)}/\lambda^{(N_{it})}$  are of the order of 10 on average in the numerical test case, while they are of the order of  $10^3$  in the experimental validation. This therefore illustrates the need for updating the regularization parameter throughout the iterative process in order to optimally adjust the amount of regularization.

Finally, to give a comprehensive overview of the overall performances

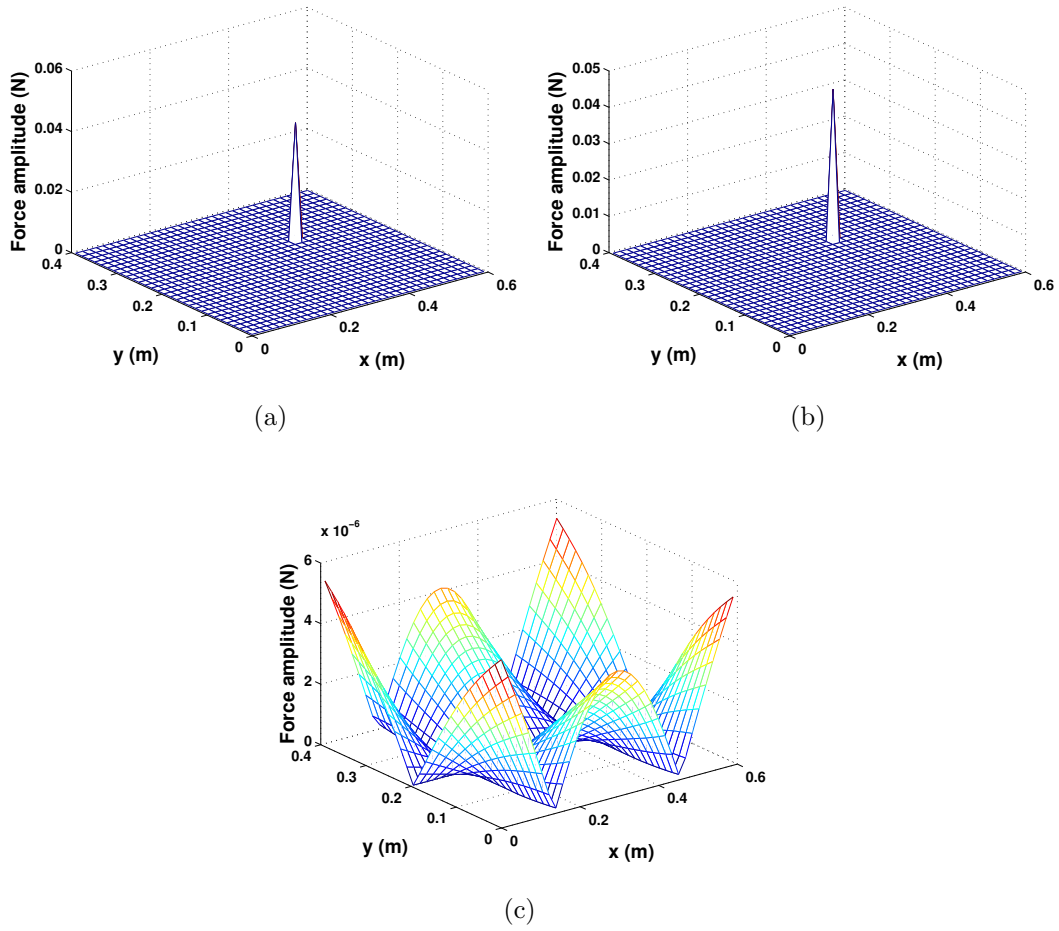


Figure 10: Comparison of additive and multiplicative regularization strategies at 196.25 Hz from the same measured data, the same tuning parameters  $q = 0.5$  and the same differentiation matrix  $\mathbf{L} = \mathbf{I}$  - (a) Multiplicative regularization, (b) Updated additive regularization and (c) Non-updated additive regularization

Table 5: Comparison of the multiplicative regularization and the additive regularizations -  $F_0$ : Target point force amplitude (mN),  $F_{i0}$ : identified point force amplitude (mN),  $N_{it}$ : number of iterations,  $t_e$ : elapsed time (s)

Frequency	$F_0$	Mult. reg.			Updated add. reg.			Non-updated add. reg.		
		$F_{m0}$	$N_{it}$	$t_e$	$F_{a0}$	$N_{it}$	$t_e$	$F_{a0}$	$N_{it}$	$t_e$
196.25 Hz	38	39	191	84	41	36	180	$5 \cdot 10^{-3}$	7	9
725 Hz	42	42	21	11	45	33	140	$6 \cdot 10^{-6}$	4	5
1161.25 Hz	52	55	40	17	56	45	202	$3 \cdot 10^{-4}$	5	6
1500 Hz	19	19	30	14	18	78	363	$5 \cdot 10^{-7}$	4	5

of the proposed multiplicative strategy, the force spectrum identified at the point force location is compared in Fig. 11 with that measured by the force sensor between 10 Hz and 1500 Hz with a frequency resolution of 1.25 Hz. For the sake of completeness, the spectrum of the point force obtained from the updated additive regularization is plotted on the same figure.

Before analyzing the results presenting in Fig. 11, it should be noted that the multiplicative regularization has required 7 hours to reconstruct the force spectrum, while the updated additive regularization has ended the reconstruction process in 78 hours. As previously observed, the multiplicative regularization is 10 times faster than its additive counterpart. But, more interestingly, the analysis of the reconstructed force spectrum leads to two main conclusions. First, the multiplicative and updated additive regularizations largely underestimate the force amplitude at certain resonance frequencies, while the reconstruction is satisfactory elsewhere. This contrasted result is

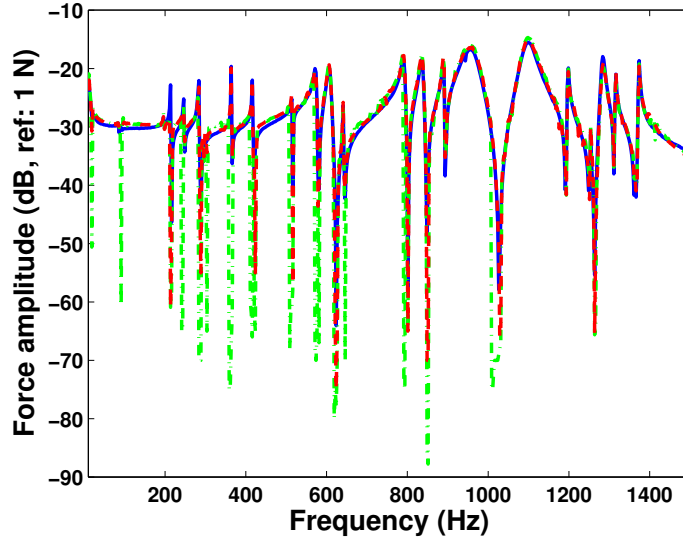


Figure 11: Reconstruction of the force spectrum - (—) Reference measured by the force sensor, (---) Multiplicative regularization and (-·-) Updated additive regularization

partly related to modelling errors insofar as the finite element model has not been updated from the measured FRFs. Second, it is worth noting that both regularization strategies behave rather differently around resonance frequencies. Indeed, it is observed that the multiplicative approach generally provides more consistent reconstructions.

## 7. Conclusion

In the vast majority of the studies dedicated to the force reconstruction problem, additive regularization strategies are implemented. Such methods require the appropriate selection of a regularization parameter before computing the regularized solution. However, this task can be computationally intensive. To bypass this potential undesirable feature of additive

approaches, a multiplicative strategy has been proposed in the present paper. From a theoretical standpoint, its main merit is to iteratively adapt the amount of regularization with respect to the problem under consideration. As a result, the optimal regularization parameter does not need to be determined at preliminary stages of the reconstruction process. Another interesting feature of the proposed approach is the definition of a multiplicative regularization term, that allows properly exploiting one’s prior knowledge of the nature and the location of the forces acting on a structure. The combination of the aforementioned characteristics makes the present multiplicative approach suitable for force reconstruction problems, as highlighted by the proposed numerical and experimental validations. These validations have also been an opportunity to compare the multiplicative strategy with related additive regularizations. In particular, the practical interest of updating the regularization parameter during the identification process has been pointed out, as well as the relative performances of the multiplicative approach in terms of computation time and reconstruction capabilities.

### **Appendix A. Derivation of the explicit form of the multiplicative regularization**

The purpose of this appendix is to detail the calculation leading to Eq. (6), as it is a key point of this work. For this purpose, one has to remind that one seeks the solution  $\mathbf{F}_m$  rendering stationary the functional:

$$J_m(\mathbf{F}) = \|\mathbf{X} - \mathbf{H}\mathbf{F}\|_2^2 \cdot \|\mathbf{F}\|_2^2. \quad (\text{A.1})$$

Practically, this is performed by applying the first-order optimality con-

dition [see Eq. (5)], namely:

$$\begin{aligned}
\left. \frac{\partial J_m(\mathbf{F})}{\partial \mathbf{F}} \right|_{\mathbf{F}=\mathbf{F}_m} &= \left. \frac{\partial \|\mathbf{X} - \mathbf{H}\mathbf{F}\|_2^2}{\partial \mathbf{F}} \right|_{\mathbf{F}=\mathbf{F}_m} \cdot \|\mathbf{F}\|_2^2 + \|\mathbf{X} - \mathbf{H}\mathbf{F}\|_2^2 \cdot \left. \frac{\partial \|\mathbf{F}\|_2^2}{\partial \mathbf{F}} \right|_{\mathbf{F}=\mathbf{F}_m} \\
&= 2 \mathbf{H}^H \mathbf{H} \mathbf{F}_m \cdot \|\mathbf{F}_m\|_2^2 - 2 \mathbf{H}^H \mathbf{X} \cdot \|\mathbf{F}_m\|_2^2 + 2 \|\mathbf{X} - \mathbf{H}\mathbf{F}_m\|_2^2 \cdot \mathbf{F}_m \\
&= \mathbf{0}.
\end{aligned} \tag{A.2}$$

After simplifying the previous equation, one has:

$$\mathbf{H}^H \mathbf{H} \mathbf{F}_m + \frac{\|\mathbf{X} - \mathbf{H}\mathbf{F}_m\|_2^2}{\|\mathbf{F}_m\|_2^2} \mathbf{F}_m = \mathbf{H}^H \mathbf{X}. \tag{A.3}$$

As a result, the solution  $\mathbf{F}_m$  is given by:

$$\mathbf{F}_m = [\mathbf{H}^H \mathbf{H} + \alpha(\mathbf{F}_m) \mathbf{I}]^{-1} \mathbf{H}^H \mathbf{X}, \quad \alpha(\mathbf{F}_m) = \frac{\|\mathbf{X} - \mathbf{H}\mathbf{F}_m\|_2^2}{\|\mathbf{F}_m\|_2^2}. \tag{A.4}$$

As a side note, it should be noticed that defining the solution of the multiplicative regularization as a stationary point of the functional  $J_m(\mathbf{F})$  leads to one obvious trivial solution, corresponding to the global minimum of the functional  $J_m(\mathbf{F})$ :

$$\mathbf{F}_m = \mathbf{0}. \tag{A.5}$$

Finally, it is also worth noting that Eq. (A.4) suggests that the least-squares solution can be approached when  $\alpha(\mathbf{F}_m) \rightarrow 0$ . When such a situation occurs, one obtains:

$$\mathbf{F}_m \approx \mathbf{H}^+ \mathbf{X}. \tag{A.6}$$

## Appendix B. Proof of the assertions given in section 2

The aim of this appendix is twofold. First, we will prove that a point of the L-curve corresponds to the solution provided by Eq. (6). Then, we will

demonstrate that the point of the L-curve given by the solution of the multiplicative regularization is the point where the tangent line to the curve has a slope equal to -1. These proofs are inspired by those given in Refs. [24, 25].

To prove that the point  $(\log \|\mathbf{X} - \mathbf{H}\mathbf{F}_m\|_2^2, \log \|\mathbf{F}_m\|_2^2)$  lies on the L-curve, let us consider  $\mathbf{F}_m$  as a stationary point of the functional  $J_m(\mathbf{F})$  given by Eq. (A.1). Let us consider now  $\mathbf{F}_a(\lambda)$  as the minimizer of the functional defining the classical Tikhonov regularization, namely:

$$J_a(\mathbf{F}, \lambda) = \|\mathbf{X} - \mathbf{H}\mathbf{F}\|_2^2 + \lambda \|\mathbf{F}\|_2^2. \quad (\text{B.1})$$

For any value of the regularization parameter  $\lambda$ , a solution  $\mathbf{F}_a(\lambda)$  can be calculated, since a minimizer of  $J_a(\mathbf{F}, \lambda)$  is given by:

$$\mathbf{F}_a(\lambda) = [\mathbf{H}^H \mathbf{H} + \lambda \mathbf{I}]^{-1} \mathbf{H}^H \mathbf{X}. \quad (\text{B.2})$$

From the foregoing, it comes that  $\mathbf{F}_m$  is a minimizer of  $J_a(\mathbf{F}, \lambda)$  for  $\lambda = \alpha(\mathbf{F}_m)$ . Consequently, the point  $(\log \|\mathbf{X} - \mathbf{H}\mathbf{F}_m\|_2^2, \log \|\mathbf{F}_m\|_2^2)$  lies on the L-curve.

Knowing that the solution of the multiplicative regularization defines a point of the L-curve, it is now possible to show that this point is the point of intersection between the L-curve and the tangent line with a slope equal to -1. To this end, it should be first remarked that  $\mathbf{F}_m$  is not only a stationary point of  $J_m(\mathbf{F})$  [see Appendix A], but also a stationary point of the functional defined by:

$$\Phi_m(\mathbf{F}) = \xi(\mathbf{F}) + \eta(\mathbf{F}), \quad (\text{B.3})$$

where  $\xi(\mathbf{F}) = \log \|\mathbf{X} - \mathbf{H}\mathbf{F}\|_2^2$  and  $\eta(\mathbf{F}) = \log \|\mathbf{F}\|_2^2$ .

By applying the first-order optimality condition to the functional  $\Phi_m(\mathbf{F})$ , it readily comes:

$$\begin{aligned} \left. \frac{\partial \Phi_m(\mathbf{F})}{\partial \mathbf{F}} \right|_{\mathbf{F}=\mathbf{F}_m} &= \left. \frac{\partial \xi(\mathbf{F})}{\partial \mathbf{F}} \right|_{\mathbf{F}=\mathbf{F}_m} + \left. \frac{\partial \eta(\mathbf{F})}{\partial \mathbf{F}} \right|_{\mathbf{F}=\mathbf{F}_m} \\ &= \left. \frac{\partial \xi(\mathbf{F})}{\partial \mathbf{F}} \right|_{\mathbf{F}=\mathbf{F}_m} \left( 1 + \left. \frac{\partial \eta(\mathbf{F})}{\partial \xi(\mathbf{F})} \right|_{\mathbf{F}=\mathbf{F}_m} \right) \\ &= \mathbf{0}. \end{aligned} \quad (\text{B.4})$$

Two situations are possible to set the previous equation to zero, since:

$$\left. \frac{\partial \xi(\mathbf{F})}{\partial \mathbf{F}} \right|_{\mathbf{F}=\mathbf{F}_m} = \mathbf{0} \quad \text{or} \quad 1 + \left. \frac{\partial \eta(\mathbf{F})}{\partial \xi(\mathbf{F})} \right|_{\mathbf{F}=\mathbf{F}_m} = 0. \quad (\text{B.5})$$

Let us consider the first situation. By using vector calculus, one finds:

$$\begin{aligned} \left. \frac{\partial \xi(\mathbf{F})}{\partial \mathbf{F}} \right|_{\mathbf{F}=\mathbf{F}_m} &= \left. \frac{\partial \log \|\mathbf{X} - \mathbf{H}\mathbf{F}\|_2^2}{\partial \mathbf{F}} \right|_{\mathbf{F}=\mathbf{F}_m} = \mathbf{0} \\ \Leftrightarrow \left. \frac{\partial \log \|\mathbf{X} - \mathbf{H}\mathbf{F}\|_2^2}{\partial \|\mathbf{X} - \mathbf{H}\mathbf{F}\|_2^2} \right|_{\mathbf{F}=\mathbf{F}_m} \cdot \left. \frac{\partial \|\mathbf{X} - \mathbf{H}\mathbf{F}\|_2^2}{\partial \mathbf{F}} \right|_{\mathbf{F}=\mathbf{F}_m} &= \mathbf{0} \\ \Leftrightarrow \frac{2}{\|\mathbf{X} - \mathbf{H}\mathbf{F}_m\|_2^2} [\mathbf{H}^H \mathbf{H}\mathbf{F}_m - \mathbf{H}^H \mathbf{X}] &= \mathbf{0}. \end{aligned} \quad (\text{B.6})$$

Consequently, the first situation leads to the least-squares solution  $\mathbf{F}_m = \mathbf{H}^+ \mathbf{X}$ .

The analysis of the second situation directly implies that:

$$\begin{aligned} \left. \frac{\partial \eta(\mathbf{F})}{\partial \xi(\mathbf{F})} \right|_{\mathbf{F}=\mathbf{F}_m} &= -1 \\ \Leftrightarrow \eta(\mathbf{F}_m) &= -\xi(\mathbf{F}_m) + C, \end{aligned} \quad (\text{B.7})$$

where  $C$  is a constant. The latter equation shows that the solution  $\mathbf{F}_m$  defines a point lying on a straight line with a slope equal to -1 and tangent to the L-curve (because  $\mathbf{F}_m$  defines a point on the L-curve as shown previously).

### Appendix C. Comparison of the running times of the proposed initialization procedure and the SVD calculation

This appendix aims at comparing the running times of the heuristic procedure proposed to estimate  $\alpha^{(0)}$  with the SVD calculation used to compute  $\lambda^{(0)}$  and  $\lambda^{(k+1)}$ . To this end, we have measured the overall running time of these operations applied to 100 realizations a random matrix  $\mathbf{A}$  of dimensions  $N \times N$  (with  $N \in [10, 10^4]$ ). Figure C.1 presents the evolution of the running times with respect to the size of the problem in log-log scale (common logarithm).

As suggested by the results presented in sections 5 and 6, the proposed heuristic procedure becomes significantly faster than the SVD calculation as the size of the problem increases. It should also be noted that for small-size problems ( $N < 70$ ), the SVD is more efficient. However, the latter observation needs to be put into perspective, since the running times are then less than 0.4 s for both calculations.

### References

- [1] M. Green. Statistics of Images, the TV Algorithm of Rudin-Osher-Fatemi for Image Denoising and an Improved Denoising Algorithm. Technical report, UCLA, 2002.

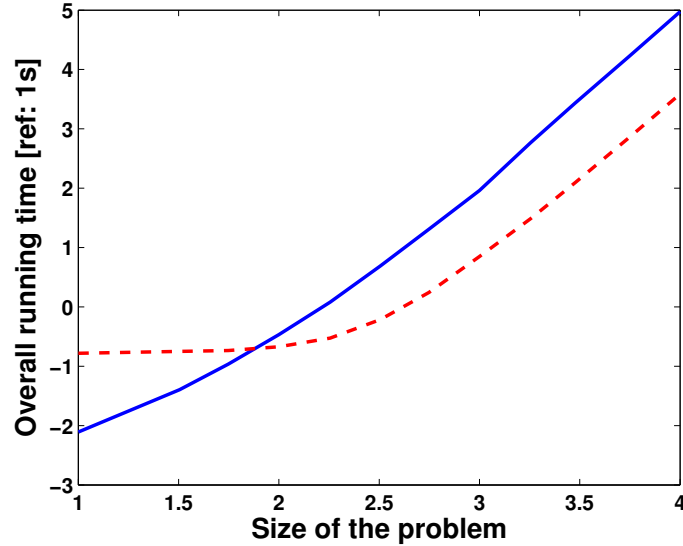


Figure C.1: Running times comparison - (—) SVD and (---) Proposed heuristic procedure

- [2] T. Le, R. Chartrand, and T. J. Asaki. A variational approach to reconstructing images corrupted by poisson noise. *Journal of Mathematical Imaging and Vision*, 27:257–263, 2007.
- [3] R. Tibshirani. Regression shrinkage and selection via the lasso. *Journal of the Royal Statistical Society*, 58 (1):267–288, 1996.
- [4] D. L. Phillips. A technique for the numerical solution of certain integral equations of the first kind. *Journal of the Association for Computing Machinery*, 9:84–97, 1962.
- [5] A. N. Tikhonov. Regularization of incorrectly posed problems. *Soviet Mathematics*, 4:1624–1627, 1963.

- [6] H. R. Busby and D. M. Trujillo. Optimal regularization of an inverse dynamics problem. *Computers & Structures*, 63 (2):243–248, 1997.
- [7] A. N. Thite and D. J. Thompson. The quantification of structure-borne transmission paths by inverse methods. Part 2 : Use of regularization techniques. *Journal of Sound and Vibration*, 264 (2):433–451, 2003.
- [8] Q. Leclere, C. Pezerat, B. Laulagnet, and L. Polac. Indirect measurement of main bearing loads in an operating diesel engine. *Journal of Sound and Vibration*, 286 (1-2):341–361, 2005.
- [9] Y. Liu and W. Steve Shepard Jr. Reducing the impact of measurement errors when reconstructing dynamic forces. *Journal of Vibration and Acoustics*, 128:586–593, 2006.
- [10] C. Renzi, C. Pezerat, and J.-L. Guyader. Vibratory source identification by using the finite element model of a subdomain of a flexural beam. *Journal of Sound and Vibration*, 332:545–562, 2013.
- [11] M. Aucejo. Structural source identification using a generalized Tikhonov regularization. *Journal of Sound and Vibration*, 333(22):5693–5707, 2014.
- [12] M. Aucejo and O. De Smet. Bayesian source identification using local priors. *Mechanical Systems and Signal Processing*, 66-67:120–136, 2016.
- [13] O. Scherzer. The use of Morozov’s discrepancy principle for Tikhonov regularization for solving nonlinear ill-posed problems. *Computing*, 51:45–60, 1993.

- [14] G. H. Golub, M. Heath, and G. Wahba. Generalized cross-validation as a method for choosing a good ridge parameter. *Technometrics*, 21 (2):215–223, 1979.
- [15] Y. Lin and B. Wohlberg. Application of the upre method to optimal parameter selection for large scale regularization problems. In *IEEE Southwest Symposium on Image Analysis and Interpretation*, Santa FE, USA, 2008.
- [16] J. Antoni. A Bayesian approach to sound source reconstruction: Optimal basis, regularization, and focusing. *Journal of the Acoustical Society of America*, 131 (4):2873–2890, 2012.
- [17] P. C. Hansen. *Rank-Deficient and Discrete Ill-Posed Problems: Numerical Aspects of Linear Inversion*. SIAM, 1998.
- [18] P. M. van den Berg, A. L. van Broekhoven, and A. Abubakar. Extended contrast source inversion. *Inverse Problems*, 15:1325–1344, 1999.
- [19] P. M. van den Berg, A. Abubakar, and J. T. Fokkema. Multiplicative regularization for constrast profile inversion. *Radio Science*, 38:8022–8031, 2003.
- [20] A. Abubakar and P. M. van den Berg. Two - and three-dimensional algorithms for microwave imaging and inverse scattering. *Journal of Electromagnetic Waves and Applications*, 17:209–231, 2003.
- [21] A. Abubakar, P. M. van den Berg, T. M. Habashy, and H. Braunish. A multiplicative regularization approach for deblurring problems. *IEEE Transactions on Image Processing*, 13:1524–1532, 2004.

- [22] A. Abubakar, P. M. van den Berg, and T. M. Habashy. An integral equation approach for 2.5-dimensional forward and inverse electromagnetic scattering. *Geophysics Journal International*, 165:744–762, 2006.
- [23] L. L. Li and B. Jafarpour. Effective solution of nonlinear subsurface flow inverse problems in sparse bases. *Inverse Problems*, 26:105016 (1–24), 2010.
- [24] J. A. Orozco Rodriguez. *Regularization for inverse problems*. PhD thesis, University of Minnesota, 2011.
- [25] T. Reginska. A regularization parameter in discrete ill-posed problems. *SIAM J. Sci. Comput.*, 17:740–749, 1996.
- [26] S. Oraintara, W. C. Karl, D. A. Castanon, and T. Q. Nguyen. A method for choosing the regularization parameter in generalized tikhonov regularized linear inverse problems. In *2000 International Conference on Image Processing*, 2000.
- [27] F. S. Viloche Bazan and J. B. Francisco. An improved fixed-point algorithm for determining a Tikhonov regularization parameter. *Inverse Problems*, 25:045007 (1–16), 2009.
- [28] P. C. Hansen. *Discrete Inverse Problems: Insight and Algorithms*. SIAM, 2010.
- [29] Wolfgang Stephan. *Total variation regularization for linear ill-posed inverse problems: Extensions and applications*. PhD thesis, Arizona State University, 2008.

- [30] P. Rodriguez and B. Wohlberg. Efficient minimization method for a generalized total variation functional. *IEEE Transactions on Image Processing*, 18 (2):322–332, 2009.
- [31] R. A. Horn and C. R. Johnson. *Topics in Matrix Analysis*. Cambridge University Press, New York, 1991.
- [32] S.R. Ibrahim, A. Fregolent, and A. Sestieri. Structural force identification at unmeasured locations. In *Proceedings of the 14th International Modal Analysis Conference*, Dearborn, USA, 1996.